Multiparameter Gaussian quantum metrology

Rosanna Nichols,[*] Pietro Liuzzo-Scorpo,[†] Paul A. Knott,[‡] and Gerardo Adesso[§]

Centre for the Mathematics and Theoretical Physics of Quantum Non-Equilibrium Systems (CQNE), School of Mathematical Sciences,
University of Nottingham, Nottingham NG7 2RD, United Kingdom

We investigate the ultimate precision achievable in Gaussian quantum metrology. We derive general analytical expressions for the quantum Fisher information matrix and for the measurement compatibility condition, ensuring asymptotic saturability of the quantum Cramér-Rao bound, for the estimation of multiple parameters encoded in multimode Gaussian states. We then apply our results to the joint estimation of a phase shift and two parameters characterizing Gaussian phase covariant noise in optical interferometry. In such a scheme, we show that two-mode displaced squeezed input probes with optimally tuned squeezing and displacement fulfill the measurement compatibility condition and enable the simultaneous estimation of all three parameters, with an advantage over individual estimation schemes that quickly rises with increasing mean energy of the probes.

I. INTRODUCTION

The exploitation of quantum effects for enhancements in sensing and precision measurements stands as one of the linchpins of the current *quantum technology* revolution [1–10]. The applications of quantum metrology range from fundamental science, such as improving time and frequency standards [11,12], advancing the sensitivity of gravitational wave interferometry [13,14], and probing space-time parameters in quantum field theory [15,16], to more applied scenarios, such as navigation [17,18], remote sensing [6,19], thermometry [20,21], spectroscopy [22,23], super-resolution imaging [24–26], magnetic field detection for biomedical diagnostics [27,28], and plenty more to come.

In many of these settings, the problem can be modeld as the estimation of unknown parameters encoded on a probe field initialized in a continuous variable (CV) Gaussian state, i.e., a Gibbs ensemble of a quadratic Hamiltonian [29–32]. If the (unitary or noisy) channel imprinting the parameters preserves the Gaussianity of the input state, the setting is overall referred to as *Gaussian quantum metrology*. Several works analyzed instances of Gaussian quantum metrology, including the estimation of single or multiple parameters using single-mode or multimode probes [1,5,8,10,15,16,20,24–26,31–59]. However, to the best of our knowledge, no general method is yet available to benchmark the *achievable* precision in multimode multiparameter Gaussian quantum metrology.

This paper bridges such a gap. First, we develop a compact expression for the so-called quantum Fisher information matrix—which determines the precision available in quantum metrology through the quantum Cramér-Rao bound [4,60–62]—for multiparameter estimation with multimode Gaussian probes. This generalizes some partial instances from previous works [32,40–45,50,51,63] and provides a derivation independent from the fidelity formula obtained in [47] by information geometry. Second, and most importantly, we also develop a compact formula to assess *compatibility* between pairs of parameters, that is, whether a common optimal measurement exists that allows one to estimate them jointly with minimum error [55]. This solves the problem of assessing the ultimate precision truly achievable in Gaussian multiparameter estimation, and provides a practical toolbox to validate effective metrological strategies for a variety of applications. These general results are presented in Sec. III, after recalling the necessary preliminary notions in Sec. II.

As an illustration, in Sec. IV we then consider the joint estimation of a phase shift and two noise parameters specifying a generic phase covariant Gaussian channel, using two-mode Gaussian probes in an interferometric setup. This extends previous studies where either phase only, or noise only, or phase and one noise parameter were estimated [1,5,33–36,39,41,43,53,55,59]. We show that two-mode displaced squeezed probes with optimally tuned displacement and squeezing enable the simultaneous estimation of all three parameters, with an advantage over individual estimation that rapidly grows with increasing mean energy of the probes. We draw our concluding remarks in Sec. V.

II. PRELIMINARIES

A. Gaussian states and Gaussian channels

An m-mode bosonic CV system [29–32] is usually described in terms of a vector of quadrature operators $\hat{\mathbf{R}} = \{\hat{q}_1, \hat{p}_1, \ldots, \hat{q}_m, \hat{p}_m\}^\top$, which satisfy the canonical commutation relation

$$[\hat{R}_j, \hat{R}_k] = i\Omega_{jk}, \qquad (1)$$

with $\Omega = i\sigma_y^{\oplus m}$. Here and in the following, $\mathbb{1}, \sigma_x, \sigma_y, \sigma_z$ stand for the 2×2 identity and the Pauli matrices, respectively, and we adopt natural units ($\hbar = 1$). It is convenient to describe the

[*]pmxrn1@nottingham.ac.uk
[†]pmxpl2@nottingham.ac.uk
[‡]paul.knott@nottingham.ac.uk
[§]gerardo.adesso@nottingham.ac.uk

density matrix $\hat{\rho}$ of a CV system by its so-called characteristic function [32,64]

$$\chi_{\hat{\rho}}(\mathbf{r}) = \text{tr}[\hat{\rho}\hat{D}_{-\mathbf{r}}], \qquad (2)$$

where

$$\hat{D}_{-\mathbf{r}} = e^{-i\mathbf{r}^\top \Omega \hat{\mathbf{R}}} \qquad (3)$$

is the displacement operator, and $\mathbf{r} = \{q_1, p_1, \ldots, q_m, p_m\}^\top$ is a vector of $2m$ real phase space coordinates.

An m-mode Gaussian state is a CV state with Gaussian characteristic function,

$$\chi_{\hat{\rho}}(\mathbf{r}) = \exp\left[-\tfrac{1}{2}\mathbf{r}^\top \Omega V \Omega \mathbf{r} - i(\Omega\mathbf{d})^\top \mathbf{r}\right], \qquad (4)$$

and hence it is fully characterized by the first and second statistical moments of its quadrature operators, i.e., the displacement vector $\mathbf{d} = \langle\hat{\mathbf{R}}\rangle$ and the covariance matrix V with elements

$$V_{jk} = \langle\{\hat{R}_j - d_j, \hat{R}_k - d_k\}_+\rangle, \qquad (5)$$

where $\{\cdot, \cdot\}_+$ is the anticommutator, and the uncertainty principle imposes

$$V \geqslant i\Omega \qquad (6)$$

for any physical state [65]. The mean energy per mode of an m-mode Gaussian state, i.e., the expectation value of the non-interacting quadratic Hamiltonian $\hat{H} = \omega\sum_{k=1}^m(\hat{a}_k^\dagger\hat{a}_k + 1/2)$ divided by the number of modes, with $\hat{a}_k = (\hat{q}_k + i\hat{p}_k)/\sqrt{2}$, can be easily computed from the covariance matrix V and the displacement vector $\mathbf{d}$ of the state [30,31]. In units of ω, this is given by

$$\frac{\langle\hat{H}\rangle}{m} \equiv \bar{n} + \frac{1}{2} = \frac{1}{2m}\left(\text{tr}\,\frac{V}{2} + |\mathbf{d}|^2\right), \qquad (7)$$

where $\bar{n}$ is the mean number of excitations per mode.

A Gaussian channel Λ is a completely positive and trace-preserving map that transforms Gaussian states into Gaussian states [29,30,32,66–70]. When a Gaussian channel preserves the number of modes of the input state, it can be represented (up to additional displacements) by two $2m \times 2m$ real matrices, X and Y, with $Y = Y^\top$, which act on the displacement vector and the covariance matrix as

$$\begin{aligned}\mathbf{d} &\to X\mathbf{d}, \\ V &\to XVX^\top + Y,\end{aligned} \qquad (8)$$

and satisfy the complete positivity condition

$$Y + iX\Omega X^\top \geqslant i\Omega. \qquad (9)$$

The latter, for single-mode Gaussian channels, reads $Y \geqslant 0$, $\sqrt{\det Y} \geqslant |1 - \det X|$. If the matrices representing the single-mode channel are proportional to the identity, $X = \sqrt{x}\mathbb{1}, Y = y\mathbb{1}$, with scalar parameters $x, y \geqslant 0$, then the channel $\Lambda_{x,y}$ is said to be phase covariant and the complete positivity condition reduces to $y \geqslant |1 - x|$.

B. Multiparameter quantum metrology

In general, to implement an estimation protocol, one needs [3–5] a probe state $\hat{\rho}_0$; a physical mechanism described by a completely positive and trace-preserving map $\Lambda_{\{\mu\}}$ which encodes, on the probe state, the set of parameters $\{\mu\}$ one wishes to estimate; and a measurement of the transformed state

$\hat{\rho}_{\{\mu\}} = \Lambda_{\{\mu\}}[\hat{\rho}_0]$ and classical postprocessing of the measurement results. This procedure allows one to construct an estimator $\{\tilde{\mu}\}$ of the unknown parameters $\{\mu\}$, whose performance is quantified by the covariance matrix cov($\{\tilde{\mu}\}$). Its diagonal elements, the variances, quantify the error in the estimation of the individual parameters, while the off-diagonal elements give an indication of the correlations between the parameters. The quantum Cramér-Rao bound yields a lower bound to the covariance matrix of an unbiased estimator in terms of the quantum Fisher information (QFI) matrix $\mathcal{F}$ [4,60–62]:

$$\text{cov}(\{\tilde{\mu}\}) \geqslant (M\mathcal{F})^{-1}, \qquad (10)$$

where M is the number of repetitions of the experiment.

In order to calculate the QFI matrix, one can introduce the symmetric logarithmic derivative (SLD) operators $\{\hat{\mathcal{L}}_\zeta\}_{\zeta\in\{\mu\}}$ which are implicitly defined by the equation

$$\hat{\mathcal{L}}_\zeta\hat{\rho}_{\{\mu\}} + \hat{\rho}_{\{\mu\}}\hat{\mathcal{L}}_\zeta = 2\frac{\partial\hat{\rho}_{\{\mu\}}}{\partial\zeta}. \qquad (11)$$

These operators are Hermitian, $\hat{\mathcal{L}}_\zeta = \hat{\mathcal{L}}_\zeta^\dagger$, by construction. The QFI matrix elements are then given by

$$\mathcal{F}_{\eta\zeta} \equiv \tfrac{1}{2}\text{tr}(\hat{\rho}_{\{\mu\}}\{\hat{\mathcal{L}}_\eta, \hat{\mathcal{L}}_\zeta\}_+) = \text{Re}[\text{tr}(\hat{\rho}_{\{\mu\}}\hat{\mathcal{L}}_\eta\hat{\mathcal{L}}_\zeta)]. \qquad (12)$$

The Cramér-Rao bound, Eq. (10), can be saturated, in the limit $M \gg 1$ of an asymptotically large number of repetitions of the protocol, if an optimal measurement can be performed on the evolved state. For each parameter, an optimal measurement is described by a set of projectors which commute with its SLD. This implies that, if $[\hat{\mathcal{L}}_\eta, \hat{\mathcal{L}}_\zeta] = 0$, then the existence of a common eigenbasis for the two SLDs is ensured, hence a jointly optimal measurement for extracting information on both parameters η and ζ can be found. However, this condition is sufficient but not necessary. A weaker condition [8,55,62,71–75] states that the multiparameter Cramér-Rao bound can be asymptotically saturated iff all pairs of SLDs commute "on average": (i) $\mathcal{J}_{\eta\zeta} = 0 \; \forall \eta, \zeta \in \{\mu\}$, with

$$\mathcal{J}_{\eta\zeta} \equiv \frac{1}{2i}\text{tr}(\hat{\rho}_{\{\mu\}}[\hat{\mathcal{L}}_\eta, \hat{\mathcal{L}}_\zeta]) = \text{Im}[\text{tr}(\hat{\rho}_{\{\mu\}}\hat{\mathcal{L}}_\eta\hat{\mathcal{L}}_\zeta)]. \qquad (13)$$

Moreover, if one wishes to estimate each parameter as precisely as one would estimate them individually when assuming perfect knowledge of the other parameters, then two more conditions need to be satisfied: (ii) there must exist a single probe state $\hat{\rho}_0$ that yields the optimal QFI for each of the parameters, and (iii) the parameters must be statistically independent, i.e., $\mathcal{F}_{\eta\zeta} = 0 \forall\eta \neq \zeta$. The latter condition ensures that the uncertainty on one parameter does not affect the estimation precision of the others. When all conditions (i)–(iii) are met, then the parameters are said to be *compatible* [55].

Estimating $\kappa \equiv |\{\mu\}|$ parameters individually, where each parameter is estimated using the state $\hat{\rho}_0$, requires κ times more resources (e.g., energy, coherence, or entanglement in the input state preparation [10,55]) than estimating them simultaneously using $\hat{\rho}_0$ in one shot; however, the latter strategy may not always offer superior performance if not all the parameters are compatible. A useful quantity to get a quantitative comparison of metrological performance between individual and

simultaneous schemes is the ratio [76]

$$\mathcal{R} = \frac{\Delta^{\text{ind}}}{\Delta^{\text{sim}}}, \qquad (14)$$

where (considering a single repetition, $M = 1$):

$$\Delta^{\text{ind}} = \sum_{\eta \in \{\mu\}} \mathcal{F}_{\eta\eta}^{-1} \quad \text{and} \quad \Delta^{\text{sim}} = \kappa^{-1} \operatorname{tr}(\mathcal{F}^{-1}) \qquad (15)$$

are the minimal total variances in the individual and simultaneous cases, respectively. Here the factor of κ^{-1} is needed to account for the fact that the simultaneous scheme requires κ less resources than individually estimating each parameter resetting the probe each time. When $\mathcal{R} > 1$, simultaneous estimation is advantageous over individual, with a maximum advantage $\mathcal{R} = \kappa$ reachable only when condition (iii) holds.

III. GAUSSIAN QUANTUM METROLOGY

Given an m-mode Gaussian state $\hat{\rho}_{\{\mu\}}$, depending on the set of parameters $\{\mu\}$, and denoting in what follows $\partial_{\cdot} \equiv \partial \cdot /\partial \zeta$, the SLD $\hat{\mathcal{L}}_\zeta$ for one of the parameters $\zeta \in \{\mu\}$ can be written as [32]

$$\hat{\mathcal{L}}_\zeta \equiv L_\zeta^{(0)} + \mathbf{L}_\zeta^{(1)\top}\hat{\mathbf{R}} + \hat{\mathbf{R}}^\top L_\zeta^{(2)}\hat{\mathbf{R}}, \qquad (16)$$

with $L_\zeta^{(0)} = -\frac{1}{2}\operatorname{tr}(V_{\{\mu\}}L_\zeta^{(2)}) - \mathbf{L}_\zeta^{(1)\top}\mathbf{d}_{\{\mu\}} - \mathbf{d}_{\{\mu\}}^\top L_\zeta^{(2)}\mathbf{d}_{\{\mu\}}$, (17)

$$\mathbf{L}_\zeta^{(1)} = 2V_{\{\mu\}}^{-1}\partial_\zeta\mathbf{d}_{\{\mu\}} - 2L_\zeta^{(2)}\mathbf{d}_{\{\mu\}}, \qquad (18)$$

$$L_\zeta^{(2)} = \sum_{j,k=1}^m \sum_{l=0}^3 \frac{(a_\zeta)_l^{jk}}{\nu_j \nu_k - (-1)^l} S^{\top -1} M_l^{jk} S^{-1}. \qquad (19)$$

In the formulas above, $\{\nu_i\}$ are the symplectic eigenvalues of the covariance matrix $V_{\{\mu\}}$, S^{-1} is the symplectic transformation that brings $V_{\{\mu\}}$ into its diagonal form,

$$S^{-1}V_{\{\mu\}}S^{\top -1} = \boldsymbol{\nu}_{\{\mu\}} = \bigoplus_{i=1}^m \nu_i \mathbb{1},$$

and

$$(a_\zeta)_l^{jk} = \operatorname{tr}(S^{-1}\partial_\zeta V_{\{\mu\}}S^{\top -1} M_l^{jk}),$$

where the set of matrices M_l^{jk} have all zero entries except for the 2×2 block in position jk which is given by

$$\{M_l^{jk}\}_{l \in \{0,\dots,3\}} = \frac{1}{\sqrt{2}}\{i\sigma_y, \sigma_z, \mathbb{1}, \sigma_x\}.$$

As the main result of this paper, we obtain the following.

Theorem 1: Given a CV bosonic Gaussian state of an arbitrary number of modes m, described by its first and second statistical moments $\mathbf{d}_{\{\mu\}}$ and $V_{\{\mu\}}$, respectively, and depending on the set of parameters $\{\mu\}$, we have for any $\eta, \zeta \in \{\mu\}$ that

$$\mathcal{F}_{\eta\zeta} = \frac{1}{2}\operatorname{tr}\big[(\partial_\zeta V_{\{\mu\}})L_\eta^{(2)}\big] + 2\big(\partial_\eta\mathbf{d}_{\{\mu\}}^\top\big)V_{\{\mu\}}^{-1}(\partial_\zeta\mathbf{d}_{\{\mu\}}), \quad (20)$$

$$\mathcal{J}_{\eta\zeta} = 2\operatorname{tr}\big(\Omega L_\zeta^{(2)}V_{\{\mu\}}L_\eta^{(2)}\big) + 2\big(\partial_\eta\mathbf{d}_{\{\mu\}}^\top\big)V_{\{\mu\}}^{-1}\Omega V_{\{\mu\}}^{-1}(\partial_\zeta\mathbf{d}_{\{\mu\}}), \qquad (21)$$

with $L_\zeta^{(2)}$ defined by Eq. (19).

Equation (20) provides a compact expression for the QFI matrix in Gaussian quantum metrology, directly generalizing

the formula for the single-parameter case which can be found, e.g., in [10,32]. Equation (21), on the other hand, provides a general formula for the quantity defined in Eq. (13), which determines the measurement compatibility condition (i) between pairs of parameters [55]. The proof of Theorem 1 is given in Appendix A. Note that, while a formula equivalent to Eq. (20) may be alternatively derived from the expression for the quantum fidelity between two Gaussian states as recently reported in [47], the formula in Eq. (21) is entirely original in the context of Gaussian quantum metrology and, to the best of our knowledge, no similar expression can be found in previous literature; in particular [77], Eq. (21) cannot be derived using the information geometry methods of [47].

Let us remark that both formulas appearing in Theorem 1 can be evaluated efficiently for an arbitrary Gaussian state $\hat{\rho}_{\{\mu\}}$, although one needs to determine explicitly the symplectic transformation S^{-1} that diagonalizes the covariance matrix $V_{\{\mu\}}$. The latter transformation can be constructed analytically for one and two modes (see, e.g., [78–80]), and in general can be obtained numerically for a higher number of modes.

IV. APPLICATION TO NOISY OPTICAL INTERFEROMETRY

To illustrate the usefulness of our results, we apply the general formalism of Theorem 1 to the technologically relevant task of quantum phase estimation under noise in optical interferometry [1,2,5,8,81,82]. We focus specifically on the scheme of Fig. 1, where an initial two-mode displaced squeezed state (TMDSS) $\hat{\rho}_0$ undergoes a phase transformation and transmission noise in an interferometric setup, before the two modes are jointly measured. Here, we define the TMDSS as having

$$\mathbf{d}_0 = \sqrt{2}\{\operatorname{Re}[\alpha], \operatorname{Im}[\alpha], \operatorname{Re}[\beta], \operatorname{Im}[\beta]\}^\top,$$

$$V_0 = \begin{pmatrix} \cosh(2r) & 0 & \sinh(2r) & 0 \\ 0 & \cosh(2r) & 0 & -\sinh(2r) \\ \sinh(2r) & 0 & \cosh(2r) & 0 \\ 0 & -\sinh(2r) & 0 & \cosh(2r) \end{pmatrix},$$

(22)

where $\alpha, \beta \in \mathbb{C}$ are the displacements of each mode, and $r \in \mathbb{R}$ is the squeezing parameter. The phase difference ϕ is imprinted by each mode undergoing a unitary shift of $\pm\phi/2$, while the noise takes the form of a generic phase covariant Gaussian
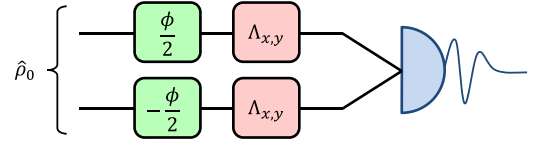

FIG. 1. An instance of multiparameter Gaussian quantum metrology. The initial state $\hat{\rho}_0$ is a two-mode displaced squeezed state which passes through an interferometric setup before a joint measurement is made. One mode undergoes a phase transformation of $\phi/2$ and the other of $-\phi/2$, while both modes are affected by a phase covariant Gaussian channel $\Lambda_{x,y}$ with noise parameters x and y. We determine optimal strategies for the estimation of the three parameters $\{\phi, x, y\}$.

channel, $\Lambda_{x,y}$, on each mode. This includes the combined effect of loss ($0 \leqslant x \leqslant 1$), amplification ($x \geqslant 1$), and added thermal noise ($y \geqslant |1-x|$), modeling realistic transmission of the probes in free space or over telecommunication fibres [29,30,32,66–70]. Our goal is to determine the best strategy to estimate all three parameters ϕ, x, and y [83], hence tracking both signal (ϕ) and noise (x, y) as precisely and efficiently as possible, using affordable TMDSS probes.

We first consider under which circumstances the compatibility condition (i) is obeyed, that is, when there exists a single optimal measurement for extracting all of the parameters such that the quantum Cramér-Rao bound (10) may be asymptotically saturated. Using Eq. (21), one can easily show that this condition becomes dependent only on the displacement of the state, reading $|\alpha|^2 = |\beta|^2$. Further examining when a TMDSS (22) leads to minimal total variances, Δ^{ind} and Δ^{sim} [see Eq. (15)], we find that optimal states minimizing both of these quantities (assuming without loss of generality $r \geqslant 0$) must have $\text{Re}[\alpha] = \text{Re}[\beta] = 0$ and $\text{Im}[\alpha] = \text{Im}[\beta]$. Consequently, any optimal input TMDSS already automatically obeys the measurement compatibility condition (i).

We can then compare individual versus simultaneous estimation schemes at fixed input mean energy, customarily regarding the latter as the main resource for the metrological protocol [4–7]. The mean energy per mode of a TMDSS (22) with $|\alpha|^2 = |\beta|^2$ can be written as $\langle \hat{H} \rangle / 2 = \bar{n} + 1/2$, with

$$\bar{n} = \sinh^2(r) + |\alpha|^2. \tag{23}$$

We find that the proportion $p \equiv |\alpha|^2 / \bar{n}$ of this energy that is optimal to invest in displacement rather than squeezing varies with x and y (but not ϕ) as well as with the total $\bar{n}$. Said optimal proportion p_{opt}, in regimes of lower and higher input mean energy, is plotted in Fig. 2 (top) against the values of parameters x and y. We observe that, at low energy, the individual and simultaneous schemes differ significantly. The optimal state for minimizing Δ_{ind} has all of its energy dedicated to displacement, whereas for simultaneous estimation all energy should be put into displacement for $x \to 0$ and the optimal proportion p_{opt} decreases from 1 as x increases, eventually dropping below $1/2$, in which case it is beneficial to put more energy in squeezing than displacement. As the available input energy $\bar{n}$ increases, this behavior quickly changes: the values of p_{opt} for the individual and simultaneous schemes become very similar. In both cases, it is always beneficial to put more energy into displacement than squeezing, with p_{opt} approaching, but never crossing, the plane $p_{\text{opt}} = 1/2$. In both strategies, there is a region of parameters at low x where the optimal input state has all its energy in displacement.

The middle and bottom rows of Fig. 2 both compare the minimal achievable total variances $\Delta^{\text{ind}}_{\text{opt}}$ and $\Delta^{\text{sim}}_{\text{opt}}$ for individual and simultaneous estimation, as defined in Eq. (15) with $\kappa = 3$ in our scheme. Specifically, the middle row shows how each variance changes with the noise parameters, while the bottom row illustrates the performance ratio $\mathcal{R}$ defined in Eq. (14). At low input energy, there are distinct regions of the parameter space where either the individual estimation scheme ($\mathcal{R} < 1$) or the simultaneous scheme ($\mathcal{R} > 1$) is preferable. The solid (red) line in Fig. 2 (bottom, left) shows the boundary between these two regions. As the energy $\bar{n}$ approaches zero, this line approaches the vertical line $x = 1$, i.e., the boundary

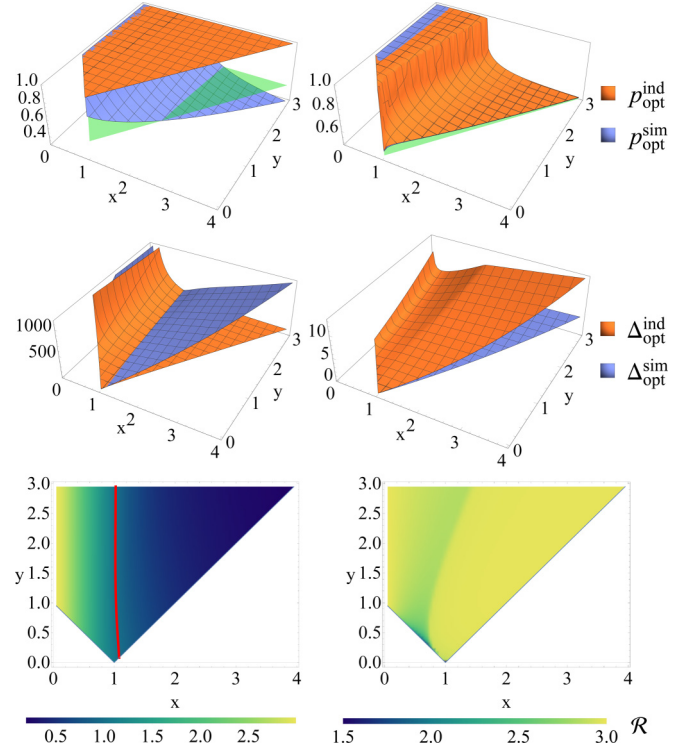FIG. 2. Results obtained from the metrological scheme outlined in Fig. 1. Left column: Analysis at low energy, $\bar{n} = 0.005$. Right column: Analysis at higher energy, $\bar{n} = 5$. Top: Optimal proportion of input energy to put in the displacement, p_{opt}, comparing individual and simultaneous estimation schemes. The unmeshed (green online) plane marks $p_{\text{opt}} = 1/2$, above which more energy should be used for displacement than squeezing. Middle: Minimal achievable error Δ_{opt} for the two strategies. Bottom: Performance ratio $\mathcal{R} = \Delta^{\text{ind}}_{\text{opt}} / \Delta^{\text{sim}}_{\text{opt}}$. The solid (red online) line marks $\mathcal{R} = 1$; when $\mathcal{R} > 1$, the simultaneous estimation scheme outperforms the individual one. All the presented results are independent of the value of the unknown phase ϕ. All the quantities plotted are dimensionless.

between loss (where simultaneous estimation is superior) and amplification channels (where individual prevails instead). As the available energy $\bar{n}$ increases, this boundary moves quickly to the right, such that for any reasonable values of the parameters one gets simultaneous estimation as the optimal scheme. In fact, as Fig. 2 (bottom, right) shows, $\mathcal{R}$ then approaches its maximum value 3 in a wide region of the parameter space. This shows that all three parameters become very nearly statistically independent, eventually fulfilling the compatibility condition (iii), with increasing input energy $\bar{n}$ [84]. Quantitatively, by a series expansion we find that in the limit $\bar{n} \gg 0$ the ratio converges to

$$\mathcal{R} \approx 3 \left[1 - \frac{(x^2 + y^2 + 1)^2}{4x^3 y} \bar{n}^{-3} + O(\bar{n}^{-4}) \right]. \tag{24}$$

We further observe that both individual and simultaneous total variances display at best a standard quantum limit scaling with the input energy, $\Delta^{\text{ind,sim}}_{\text{opt}} \lesssim O(\bar{n}^{-1})$, with no sub-shot-noise enhancement possible due to the presence of noise, in agreement with the general predictions of Refs. [59,81,82]. For completeness, the explicit QFI matrix $\mathcal{F}$ for the three pa-

rameters $\{\phi, x, y\}$, as computed from Eq. (20) using optimized TMDSS probes, is reported in Appendix B. We finally note that, in the individual estimation scheme, we have determined an optimal input state that minimizes the total variance Δ^{ind} as defined in Eq. (15), but one could, in principle, consider a different input state optimized independently for the estimation of each parameter. This analysis, also reported in Appendix B, leads to slightly better performances for individual estimation, but does not change any of the conclusions discussed above, including the fulfillment of the compatibility conditions and the qualitative regime where simultaneous estimation is advantageous.

V. CONCLUSIONS

In this paper we derived general formulas to assess the ultimate precision available in Gaussian quantum metrology, that is, in the estimation of multiple parameters encoded in multimode Gaussian quantum states [32]. We derived a compact expression, in terms of first and second moments of the states, for the quantum Fisher information matrix, which bounds the achievable estimation error via the quantum Cramér-Rao bound. We then obtained a compact analytical expression to assess iff such a bound can be asymptotically saturated, i.e., iff a common measurement exists that is able to extract information optimally on all the parameters, a condition known as measurement compatibility [55]. This yields a general tool to endorse feasible estimation strategies in multiparameter Gaussian quantum metrology.

We applied our general formalism to study the practical estimation of three relevant physical parameters in noisy optical interferometry: an unknown phase shift and two unknown noise terms which specify a generic phase covariant Gaussian channel, capturing realistic instances of imperfect transmission. We showed that, using two-mode displaced squeezed input probes with optimally tuned squeezing and displacement, the measurement compatibility condition is satisfied, and one can estimate all three parameters simultaneously with an advantage over individual schemes growing rapidly as the available input energy is increased, eventually reaching a regime where the parameters are *de facto* statistically independent.

Our techniques can be promptly applied to a broad range of problems in fundamental science and technology [4–6], including (gravitational) interferometry, biosensing, imaging, positioning, thermometry, and more generally wherever the precise estimation of parameters encoded in quadratic Hamiltonians or noisy evolutions preserving Gaussianity is demanded. While this work focused mainly on compatibility conditions (i) and (iii), i.e., measurement compatibility and statistical independence [55], our framework can be combined with efficient numerical algorithms to find optimal input probe states [50,85,86], in order to fulfill condition (ii) and minimize the overall error on estimating multiple parameters. Tailoring existing algorithms—or devising new ones—to search within multimode Gaussian states, constrained to the compatibility constraints derived here, may be a valuable next step.

Note added. Recently, an independent derivation of Eq. (20) was reported by D. Šafránek in [87].

APPENDIX A: PROOF OF THEOREM 1

To prove Theorem 1 we will calculate explicitly, term by term, the following expression [adopting the notation $\mathbf{L}_\eta^{(1)} = (L_{\eta\, l}^{(1)})$ and $L_\eta^{(2)} = (L_{\eta\, jk}^{(2)})$, for $j,k,l \in \{1, \ldots, m\}$, and assuming here and in the following a sum over repeated indices]:

$$\text{tr}(\hat{\rho}_{\{\mu\}}\hat{\mathcal{L}}_\eta\hat{\mathcal{L}}_\zeta) = \text{tr}\left[\hat{\rho}_{\{\mu\}}\left(L_\eta^{(0)} + L_{\eta\, l}^{(1)}\hat{R}_l + L_{\eta\, jk}^{(2)}\hat{R}_j\hat{R}_k\right)\left(L_\zeta^{(0)} + L_{\zeta\, m}^{(1)}\hat{R}_m + L_{\zeta\, pq}^{(2)}\hat{R}_p\hat{R}_q\right)\right],$$

i.e., we will find the explicit expressions for $\text{tr}(\hat{\rho}_{\{\mu\}}\hat{R}_p\hat{R}_q)$, $\text{tr}(\hat{\rho}_{\{\mu\}}\hat{R}_l\hat{R}_p\hat{R}_q)$, and $\text{tr}(\hat{\rho}_{\{\mu\}}\hat{R}_j\hat{R}_k\hat{R}_p\hat{R}_q)$; recall that the linear term is just the displacement vector: $\text{tr}(\hat{\rho}_{\{\mu\}}\hat{R}_l) = d_l$.

We will make use of some properties of the symmetrically ordered characteristic function $\chi(\mathbf{r})$. The first property is that the expectation value of an operator is equal to the characteristic function associated to it evaluated in $\mathbf{r} = 0$. The second one is that given any bounded operator $\hat{O}$, the following holds as a consequence of the Baker-Campbell-Hausdorff decomposition of the displacement operator:

$$\chi_{\hat{O}\hat{R}_j}(\mathbf{r}) = \text{Tr}[\hat{D}_{-\mathbf{r}}\hat{O}\hat{R}_j] = \left(-i\frac{\partial}{\partial\tilde{r}_j} - \frac{1}{2}\Omega_{jk}\tilde{r}_k\right)\chi_{\hat{O}}(\mathbf{r}), \tag{A1}$$

where $\tilde{\mathbf{r}} = \Omega\mathbf{r}$. The last property we use reads

$$\frac{\partial}{\partial\tilde{r}_m}\chi_{\hat{\rho}_{\{\mu\}}} = \frac{\partial}{\partial\tilde{r}_m}e^{-(1/4)\tilde{r}_k V_{\{\mu\},kj}\tilde{r}_j + i d_{\{\mu\},l}\tilde{r}_l} = i d_{\{\mu\},m} - \frac{1}{2}V_{\{\mu\},mj}\tilde{r}_j, \tag{A2}$$

and it follows directly from the definition (4) of Gaussian characteristic function:

$$\chi_{\hat{\rho}_{\{\mu\}}}(\mathbf{r}) = \exp\left[-\frac{1}{2}\mathbf{r}^\top \Omega V_{\{\mu\}} \Omega \mathbf{r} - i(\Omega \mathbf{d}_{\{\mu\}})^\top \mathbf{r}\right]. \tag{A3}$$

In the rest of the proof, for the sake of a lighter notation, we will indicate with $\chi \equiv \chi_{\hat{\rho}_{\{\mu\}}}$ the symmetrically ordered characteristic function of the Gaussian state $\hat{\rho}_{\{\mu\}}$ (if not specified otherwise) and we will write ∂_j for $\frac{\partial}{\partial \tilde{r}_j}$. Moreover, we will drop the explicit dependence on the set of parameters $\{\mu\}$ from $\boldsymbol{d}_{\{\mu\}}$ and $V_{\{\mu\}}$, that is, we will use the shortcuts $d_j \equiv (\boldsymbol{d}_{\{\mu\}})_j \equiv d_{\{\mu\},j}$ and $V_{jk} \equiv (V_{\{\mu\}})_{jk} \equiv V_{\{\mu\},jk}$.

1. Quadratic term: $\text{tr}(\hat{\rho}_{\{\mu\}}\hat{R}_p\hat{R}_q)$

Making use of property (A1) we get

$$\text{tr}(\hat{\rho}_{\{\mu\}}\hat{R}_p\hat{R}_q) = \left(-i\partial_q - \frac{1}{2}\Omega_{qq'}\tilde{r}_{q'}\right)\chi_{\hat{\rho}_{\{\mu\}}\hat{R}_q}\bigg|_{\tilde{\mathbf{r}}=\mathbf{0}} = \left(-i\partial_q - \frac{1}{2}\Omega_{qq'}\tilde{r}_{q'}\right)\left(-i\partial_p - \frac{1}{2}\Omega_{pp'}\tilde{r}_{p'}\right)\chi\bigg|_{\tilde{\mathbf{r}}=\mathbf{0}}$$

$$= \left[(-i)^2\partial_q\partial_p\chi + \frac{i}{2}\Omega_{pp'}\partial_q(\tilde{r}_{p'}\chi) + \frac{i}{2}\Omega_{qq'}\tilde{r}_{q'}\partial_p\chi + \frac{1}{4}\Omega_{qq'}\Omega_{pp'}\tilde{r}_{q'}\tilde{r}_{p'}\chi\right]_{\tilde{\mathbf{r}}=\mathbf{0}}$$

$$= \left[-\partial_q\partial_p\chi + \frac{i}{2}\Omega_{pp'}(\delta_{qp'}\chi + \tilde{r}_{p'}\partial_q\chi)\right]_{\tilde{\mathbf{r}}=\mathbf{0}} = -\partial_q\partial_p\chi|_{\tilde{\mathbf{r}}=\mathbf{0}} + \frac{i}{2}\Omega_{pq}, \tag{A4}$$

and exploiting property (A2) we find

$$\partial_q\partial_p\chi = \left(id_p - \frac{1}{2}V_{pp'}\tilde{r}_{p'}\right)\partial_q\chi + \partial_q\left[\left(\left(id_p - \frac{1}{2}V_{pp'}\tilde{r}_{p'}\right)\right)\right]\chi$$

$$= \left(id_p - \frac{1}{2}V_{pp'}\tilde{r}_{p'}\right)\left(id_q - \frac{1}{2}V_{qq'}\tilde{r}_{q'}\right)\chi - \frac{1}{2}V_{pp'}\delta_{qp'}\chi$$

$$= \left(id_p - \frac{1}{2}V_{pp'}\tilde{r}_{p'}\right)\left(id_q - \frac{1}{2}V_{qq'}\tilde{r}_{q'}\right)\chi - \frac{1}{2}V_{pq}\chi. \tag{A5}$$

Evaluating this last expression in $\tilde{\mathbf{r}} = \mathbf{0}$ we get

$$\partial_q\partial_p\chi|_{\tilde{\mathbf{r}}=\mathbf{0}} = -d_pd_q - \tfrac{1}{2}V_{pq}, \tag{A6}$$

and plugging this into Eq. (A4) we finally obtain

$$\text{tr}(\hat{\rho}_{\{\mu\}}\hat{R}_p\hat{R}_q) = d_pd_q + \tfrac{1}{2}(V_{pq} + i\Omega_{pq}). \tag{A7}$$

2. Cubic term: $\text{tr}(\hat{\rho}_{\{\mu\}}\hat{R}_l\hat{R}_p\hat{R}_q)$

Applying property (A1) we write

$$\text{tr}(\hat{\rho}_{\{\mu\}}\hat{R}_l\hat{R}_p\hat{R}_q) = \left(-i\partial_q - \frac{1}{2}\Omega_{qq'}\tilde{r}_{q'}\right)\left(-i\partial_p - \frac{1}{2}\Omega_{pp'}\tilde{r}_{p'}\right)\left(-i\partial_l - \frac{1}{2}\Omega_{ll'}\tilde{r}_{l'}\right)\chi\bigg|_{\tilde{\mathbf{r}}=\mathbf{0}}$$

$$= \left[(-i)^3\partial_q\partial_p\partial_l\chi - \frac{(-i)^2}{2}\Omega_{ll'}\partial_q\partial_p(\tilde{r}_{l'}\chi) - \frac{i}{4}\Omega_{pp'}\Omega_{ll'}\partial_q(\tilde{r}_{p'}\tilde{r}_{l'}\chi)\right.$$

$$\left. - \frac{(-i)^2}{2}\Omega_{pp'}\partial_q(\tilde{r}_{p'}\partial_l\chi) - \frac{(-i)^2}{2}\Omega_{qq'}\tilde{r}_{q'}\partial_p\partial_q\chi - \frac{i}{4}\Omega_{qq'}\Omega_{ll'}\tilde{r}_{q'}\partial_p(\tilde{r}_{l'}\chi)\right.$$

$$\left. - \frac{i}{4}\Omega_{qq'}\Omega_{pp'}\tilde{r}_{q'}\tilde{r}_{p'}\partial_l\chi - \frac{1}{8}\Omega_{qq'}\Omega_{pp'}\Omega_{ll'}\tilde{r}_{q'}\tilde{r}_{p'}\tilde{r}_{l'}\chi\right]_{\tilde{\mathbf{r}}=\mathbf{0}}$$

$$= \left[i\partial_q\partial_p\partial_l\chi + \frac{1}{2}\Omega_{ll'}\partial_q\partial_p(\tilde{r}_{l'}\chi) + \frac{1}{2}\Omega_{pp'}\partial_q(\tilde{r}_{p'}\partial_l\chi)\right]_{\tilde{\mathbf{r}}=\mathbf{0}}. \tag{A8}$$

Making use of property (A2), the three terms above are readily found. When evaluated in $\tilde{\mathbf{r}} = \mathbf{0}$, they read

$$\partial_q\partial_p(\tilde{r}_{l'}\chi)|_{\tilde{\mathbf{r}}=\mathbf{0}} = id_q\delta_{pl'} + id_p\delta_{ql'},$$

$$\partial_q(\tilde{r}_{p'}\partial_l\chi)|_{\tilde{\mathbf{r}}=\mathbf{0}} = id_l\delta_{qp'},$$

$$\partial_q\partial_p\partial_l\chi|_{\tilde{\mathbf{r}}=\mathbf{0}} = -id_pd_ld_q - \frac{i}{2}(V_{pl}d_q + V_{pq}d_l + V_{lq}d_p).$$

Hence we get (notice that $V_{jk} = V_{kj}$ as the covariance matrix is symmetric)

$$\text{tr}(\hat{\rho}_{\{\mu\}}\hat{R}_l\hat{R}_p\hat{R}_q) = d_p d_l d_q + \tfrac{1}{2}[(V_{lp} + i\Omega_{lp})d_q + (V_{pq} + i\Omega_{pq})d_l + (V_{lq} + i\Omega_{lq})d_p]. \tag{A9}$$

3. Quartic term: $\text{tr}(\hat{\rho}_{\{\mu\}}\hat{R}_j\hat{R}_k\hat{R}_p\hat{R}_q)$

Considering that the linear term in $\tilde{r}_q$ gives no contribution when evaluated in $\tilde{\mathbf{r}} = \mathbf{0}$, we have

$$\text{tr}(\hat{\rho}_{\{\mu\}}\hat{R}_j\hat{R}_k\hat{R}_p\hat{R}_q) = -i\partial_q\left(-i\partial_p - \tfrac{1}{2}\Omega_{pp'}\tilde{r}_{p'}\right)\left(-i\partial_k - \tfrac{1}{2}\Omega_{kk'}\tilde{r}_{k'}\right)\left(-i\partial_j - \tfrac{1}{2}\Omega_{jj'}\tilde{r}_{j'}\right)\chi\Big|_{\tilde{\mathbf{r}}=\mathbf{0}}$$

$$= -i\partial_q\bigg[(-i)^3\partial_p\partial_k\partial_j\chi - \frac{(-i)^2}{2}\Omega_{jj'}\partial_p\partial_k(\tilde{r}_{j'}\chi) - \frac{i}{4}\Omega_{kk'}\Omega_{jj'}\partial_p(\tilde{r}_{k'}\tilde{r}_{j'}\chi)$$

$$- \frac{(-i)^2}{2}\Omega_{kk'}\partial_p(\tilde{r}_{k'}\partial_j\chi) - \frac{(-i)^2}{2}\Omega_{pp'}\tilde{r}_{p'}\partial_k\partial_j\chi - \frac{i}{4}\Omega_{pp'}\Omega_{jj'}\tilde{r}_{p'}\partial_k(\tilde{r}_{j'}\chi)$$

$$- \frac{i}{4}\Omega_{pp'}\Omega_{kk'}\tilde{r}_{p'}\tilde{r}_{k'}\partial_j\chi - \frac{1}{8}\Omega_{pp'}\Omega_{kk'}\Omega_{jj'}\tilde{r}_{p'}\tilde{r}_{k'}\tilde{r}_{j'}\chi\bigg]_{\tilde{\mathbf{r}}=\mathbf{0}}.$$

Notice that the last two terms do not contribute when evaluated in $\tilde{\mathbf{r}} = \mathbf{0}$, since they are of the second and third order in $\tilde{r}$ and, when differentiated with respect to $\tilde{r}_q$, they produce a linear and a quadratic term, respectively. We then get

$$\text{tr}(\hat{\rho}_{\{\mu\}}\hat{R}_j\hat{R}_k\hat{R}_p\hat{R}_q) = \bigg\{(-i)^4\partial_q\partial_p\partial_k\partial_j\chi - \frac{(-i)^3}{2}\Omega_{jj'}\partial_q\partial_p\partial_k(\tilde{r}_{j'}\chi)$$

$$+ \frac{(-i)^2}{4}\Omega_{kk'}\Omega_{jj'}\partial_q\partial_p(\tilde{r}_{k'}\tilde{r}_{j'}\chi) - \frac{(-i)^3}{2}\Omega_{kk'}\partial_q\partial_p(\tilde{r}_{k'}\partial_j\chi)$$

$$- \frac{(-i)^3}{2}\Omega_{pp'}\partial_q(\tilde{r}_{p'}\partial_k\partial_j\chi) + \frac{(-i)^2}{4}\Omega_{pp'}\Omega_{jj'}\partial_q\big[\tilde{r}_{p'}\partial_k(\tilde{r}_{j'}\chi)\big]\bigg\}_{\tilde{\mathbf{r}}=\mathbf{0}}. \tag{A10}$$

The six terms above, when evaluated in $\tilde{\mathbf{r}} = \mathbf{0}$, give

$$\partial_q\partial_p\partial_k(\tilde{r}_{j'}\chi)|_{\tilde{\mathbf{r}}=\mathbf{0}} = \delta_{kj'}\partial_q\partial_p\chi|_{\mathbf{r}=\mathbf{0}} + \delta_{pj'}\partial_q\partial_k\chi|_{\mathbf{r}=\mathbf{0}} + \delta_{qj'}\partial_p\partial_k\chi|_{\mathbf{r}=\mathbf{0}},$$

$$\partial_q\partial_p(\tilde{r}_{k'}\tilde{r}_{j'}\chi)|_{\tilde{\mathbf{r}}=\mathbf{0}} = \delta_{pk'}\delta_{qj'} + \delta_{pj'}\delta_{qk'},$$

$$\partial_q\partial_p(r_{k'}\partial_j\chi)|_{\tilde{\mathbf{r}}=\mathbf{0}} = \delta_{pk'}\partial_q\partial_j\chi|_{\mathbf{r}=\mathbf{0}} + \delta_{qk'}\partial_p\partial_j\chi|_{\mathbf{r}=\mathbf{0}},$$

$$\partial_q(\tilde{r}_{p'}\partial_k\partial_j\chi)|_{\tilde{\mathbf{r}}=\mathbf{0}} = \delta_{qp'}\partial_k\partial_j\chi|_{\mathbf{r}=\mathbf{0}},$$

$$\partial_q\big[\tilde{r}_{p'}\partial_k(\tilde{r}_{j'}\chi)\big]|_{\tilde{\mathbf{r}}=\mathbf{0}} = \delta_{qp'}\delta_{kj'},$$

$$\partial_q\partial_p\partial_k\partial_j\chi|_{\tilde{\mathbf{r}}=\mathbf{0}} = d_k d_j d_q d_p + \tfrac{1}{2}(V_{qp}d_k d_j + V_{kj}d_p d_q + V_{kq}d_j d_p + V_{jq}d_k d_p + V_{kp}d_j d_q + V_{jp}d_k d_q)$$

$$+ \tfrac{1}{4}(V_{kp}V_{jq} + V_{jp}V_{kq} + V_{kj}V_{qp}).$$

Plugging these expressions into Eq. (A10), we get

$$\text{tr}(\hat{\rho}_{\{\mu\}}\hat{R}_j\hat{R}_k\hat{R}_p\hat{R}_q) = d_j d_k d_p d_q + \tfrac{1}{2}d_p d_q V_{jk} + \tfrac{1}{2}d_k d_q V_{jp} + \tfrac{1}{2}d_j d_q V_{kp} + \tfrac{1}{2}d_k d_p V_{jq} + \tfrac{1}{2}d_j d_p V_{kq} + \tfrac{1}{2}d_j d_k V_{pq}$$

$$+ \frac{i}{2}\bigg\{\Omega_{jk}\left(d_p d_q + \frac{V_{pq}}{2}\right) + \Omega_{jp}\left(d_k d_q + \frac{V_{kq}}{2}\right) + \Omega_{kp}\left(d_j d_q + \frac{V_{jq}}{2}\right)$$

$$+ \Omega_{jq}\left(d_k d_p + \frac{V_{kp}}{2}\right) + \Omega_{kq}\left(d_j d_p + \frac{V_{jp}}{2}\right) + \Omega_{pq}\left(d_j d_k + \frac{V_{jk}}{2}\right)\bigg\}$$

$$- \tfrac{1}{4}(\Omega_{jq}\Omega_{kp} + \Omega_{jp}\Omega_{kq} + \Omega_{jk}\Omega_{pq}) + \tfrac{1}{4}(V_{jq}V_{kp} + V_{jp}V_{kq} + V_{jk}V_{pq}). \tag{A11}$$

Before moving to the last part of the proof, we recall that the expectation value of the SLD operator is zero. This is easy to check:

$$\langle\hat{\mathcal{L}}_\zeta\rangle = \text{tr}(\hat{\rho}_{\{\mu\}}\hat{\mathcal{L}}_\zeta) = L_\zeta^{(0)}\text{tr}(\hat{\rho}_{\{\mu\}}) + L_{\zeta\,m}^{(1)}\text{tr}(\hat{\rho}_{\{\mu\}}\hat{R}_m) + L_{\zeta\,jk}^{(2)}\text{tr}(\hat{\rho}_{\{\mu\}}\hat{R}_j\hat{R}_k)$$

$$= L_\zeta^{(0)} + L_{\zeta\,m}^{(1)}d_m + L_{\zeta\,jk}^{(2)}\left(d_j d_k + \tfrac{1}{2}(V_{jk} + i\Omega_{jk})\right),$$

which in vectorial form reads

$$\langle\hat{\mathcal{L}}_\zeta\rangle = L_\zeta^{(0)} + \mathbf{L}_\zeta^{(1)\mathsf{T}}\mathbf{d} + \mathbf{d}^\mathsf{T}L_\zeta^{(2)}\mathbf{d} + \tfrac{1}{2}\text{tr}(L_\zeta^{(2)}V) + \tfrac{i}{2}\text{tr}(L_\zeta^{(2)}\Omega). \tag{A12}$$

When substituting the definition of $L_\zeta^{(0)}$ from Eq. (17) into Eq. (A12), we are left with a term proportional to $\mathrm{tr}(L_\zeta^{(2)}\Omega)$, which vanishes because $L_\zeta^{(2)}$ is symmetric while Ω is skew-symmetric.

4. Expressions for $\mathrm{tr}(\hat{\rho}_{\{\mu\}}\hat{\mathcal{L}}_\eta\hat{\mathcal{L}}_\zeta)$, $\mathcal{F}_{\eta\zeta}$, $\mathcal{J}_{\eta\zeta}$

We have that

$$
\begin{aligned}
\mathrm{tr}\big(\hat{\rho}_{\{\mu\}}\hat{\mathcal{L}}_\eta\hat{\mathcal{L}}_\zeta\big) = {}& L_\eta^{(0)}L_\zeta^{(0)} + L_\eta^{(0)}L_{\zeta\,m}^{(1)}\mathrm{tr}(\hat{\rho}_{\{\mu\}}\hat{R}_m) + L_\eta^{(0)}L_{\zeta\,pq}^{(2)}\mathrm{tr}(\hat{\rho}_{\{\mu\}}\hat{R}_p\hat{R}_q) \\
& + L_{\eta\,l}^{(1)}L_\zeta^{(0)}\mathrm{tr}(\hat{\rho}_{\{\mu\}}\hat{R}_l) + L_{\eta\,l}^{(1)}L_{\zeta\,m}^{(1)}\mathrm{tr}(\hat{\rho}_{\{\mu\}}\hat{R}_l\hat{R}_m) + L_{\eta\,l}^{(1)}L_{\zeta\,pq}^{(2)}\mathrm{tr}(\hat{\rho}_{\{\mu\}}\hat{R}_l\hat{R}_p\hat{R}_q) \\
& + L_{\eta\,jk}^{(2)}L_\zeta^{(0)}\mathrm{tr}(\hat{\rho}_{\{\mu\}}\hat{R}_j\hat{R}_k) + L_{\eta\,jk}^{(2)}L_{\zeta\,m}^{(1)}\mathrm{tr}(\hat{\rho}_{\{\mu\}}\hat{R}_j\hat{R}_k\hat{R}_m) + L_{\eta\,jk}^{(2)}L_{\zeta\,pq}^{(2)}\mathrm{tr}(\hat{\rho}_{\{\mu\}}\hat{R}_j\hat{R}_k\hat{R}_p\hat{R}_q),
\end{aligned}
$$

and exploiting the results of the previous sections we get

$$
\begin{aligned}
\mathrm{tr}(\hat{\rho}_{\{\mu\}}\hat{\mathcal{L}}_\eta\hat{\mathcal{L}}_\zeta) = {}& L_\eta^{(0)}L_\zeta^{(0)} + L_\eta^{(0)}L_{\zeta\,m}^{(1)}d_m + L_\eta^{(0)}L_{\zeta\,pq}^{(2)}\left(d_pd_q + \frac{1}{2}(V_{pq}+i\Omega_{pq})\right) + L_{\eta\,l}^{(1)}L_\zeta^{(0)}d_l \\
& + L_{\eta\,l}^{(1)}L_{\zeta\,m}^{(1)}\left(d_ld_m + \frac{1}{2}(V_{lm}+i\Omega_{lm})\right) \\
& + L_{\eta\,l}^{(1)}L_{\zeta\,pq}^{(2)}\left(d_pd_ld_q + (V_{lp}+i\Omega_{lp})\frac{d_q}{2} + (V_{pq}+i\Omega_{pq})\frac{d_l}{2} + (V_{lq}+i\Omega_{lq})\frac{d_p}{2}\right) \\
& + L_{\eta\,jk}^{(2)}L_\zeta^{(0)}\left(d_jd_k + \frac{1}{2}(V_{jk}+i\Omega_{jk})\right) \\
& + L_{\eta\,jk}^{(2)}L_{\zeta\,m}^{(1)}\left(d_jd_kd_m + (V_{jk}+i\Omega_{jk})\frac{d_m}{2} + V_{km}+i\Omega_{km}\frac{d_j}{2} + (V_j+i\Omega_{jm})\frac{d_k}{2}\right) \\
& + L_{\eta\,jk}^{(2)}L_{\zeta\,pq}^{(2)}\Bigg\{ d_jd_kd_pd_q + \frac{1}{2}d_pd_qV_{jk} + \frac{1}{2}d_kd_qV_{jp} + \frac{1}{2}d_jd_qV_{kp} \\
& + \frac{1}{2}d_kd_pV_{jq} + \frac{1}{2}d_jd_pV_{kq} + \frac{1}{2}d_jd_kV_{pq} + \frac{1}{4}V_{jq}V_{kp} + \frac{1}{4}V_{jp}V_{kq} + \frac{1}{4}V_{jk}V_{pq} \\
& + \frac{1}{2}i\left[\Omega_{jk}\left(d_pd_q + \frac{V_{pq}}{2}\right) + \Omega_{jp}\left(d_kd_q + \frac{V_{kq}}{2}\right) + \Omega_{kp}\left(d_jd_q + \frac{V_{jq}}{2}\right) + \Omega_{jq}\left(d_kd_p + \frac{V_{kp}}{2}\right) \right. \\
& \left. + \Omega_{kq}\left(d_jd_p + \frac{V_{jp}}{2}\right) + \Omega_{pq}\left(d_jd_k + \frac{V_{jk}}{2}\right)\right] - \frac{1}{4}\big(\Omega_{jq}\Omega_{kp} + \Omega_{jp}\Omega_{kq} + \Omega_{jk}\Omega_{pq}\big)\Bigg\} \\
= {}& \frac{1}{2}d_kV_{jm}L_{\eta\,jk}^{(2)}L_{\zeta\,m}^{(1)} + \frac{1}{2}d_jL_{\eta\,jk}^{(2)}V_{km}L_{\zeta\,m}^{(1)} + \frac{1}{2}id_k\Omega_{jm}L_{\eta\,jk}^{(2)}L_{\zeta\,m}^{(1)} + \frac{1}{2}id_jL_{\eta\,jk}^{(2)}\Omega_{km}L_{\zeta\,m}^{(1)} \\
& + \frac{1}{2}d_kd_qV_{jp}L_{\eta\,jk}^{(2)}L_{\zeta\,pq}^{(2)} + \frac{1}{2}d_jd_qL_{\eta\,jk}^{(2)}V_{kp}L_{\zeta\,pq}^{(2)} + \frac{1}{2}d_kd_pV_{jq}L_{\eta\,jk}^{(2)}L_{\zeta\,pq}^{(2)} + \frac{1}{2}d_jd_pL_{\eta\,jk}^{(2)}V_{kq}L_{\zeta\,pq}^{(2)} \\
& + \frac{1}{2}id_kd_q\Omega_{jp}L_{\eta\,jk}^{(2)}L_{\zeta\,pq}^{(2)} + \frac{1}{2}id_kd_p\Omega_{jq}L_{\eta\,jk}^{(2)}L_{\zeta\,pq}^{(2)} + \frac{1}{2}id_jd_qL_{\eta\,jk}^{(2)}\Omega_{kp}L_{\zeta\,pq}^{(2)} + \frac{1}{2}id_jd_pL_{\eta\,jk}^{(2)}\Omega_{kq}L_{\zeta\,pq}^{(2)} \\
& + \frac{1}{2}d_qL_{\eta\,l}^{(1)}V_{lp}L_{\zeta\,pq}^{(2)} + \frac{1}{2}d_pL_{\eta\,l}^{(1)}V_{lq}L_{\zeta\,pq}^{(2)} + \frac{1}{2}id_qL_{\eta\,l}^{(1)}\Omega_{lp}L_{\zeta\,pq}^{(2)} + \frac{1}{2}id_pL_{\eta\,l}^{(1)}\Omega_{lq}L_{\zeta\,pq}^{(2)} \\
& + \frac{1}{4}i\Omega_{jp}L_{\eta\,jk}^{(2)}V_{kq}L_{\zeta\,pq}^{(2)} + \frac{1}{4}i\Omega_{jq}L_{\eta\,jk}^{(2)}V_{kp}L_{\zeta\,pq}^{(2)} + \frac{1}{4}iV_{jq}L_{\eta\,jk}^{(2)}\Omega_{kp}L_{\zeta\,pq}^{(2)} + \frac{1}{4}iV_{jp}L_{\eta\,jk}^{(2)}\Omega_{kq}L_{\zeta\,pq}^{(2)} \\
& + \frac{1}{4}V_{jq}L_{\eta\,jk}^{(2)}V_{kp}L_{\zeta\,pq}^{(2)} + \frac{1}{4}V_{jp}L_{\eta\,jk}^{(2)}V_{kq}L_{\zeta\,pq}^{(2)} - \frac{1}{4}\Omega_{jq}L_{\eta\,jk}^{(2)}\Omega_{kp}L_{\zeta\,pq}^{(2)} - \frac{1}{4}\Omega_{jp}L_{\eta\,jk}^{(2)}\Omega_{kq}L_{\zeta\,pq}^{(2)} \\
& + \frac{1}{2}L_{\eta\,l}^{(1)}V_{lm}L_{\zeta\,m}^{(1)} + \frac{1}{2}iL_{\eta\,l}^{(1)}\Omega_{lm}L_{\zeta\,m}^{(1)},
\end{aligned} \tag{A13}
$$

where to obtain the last equality we used the trick of subtracting $\langle\hat{\mathcal{L}}_\zeta\rangle\langle\hat{\mathcal{L}}_\eta\rangle = 0$.

In vectorial form, Eq. (A13) becomes

$$
\begin{aligned}
\mathrm{tr}\big(\hat{\rho}_{\{\mu\}}\hat{\mathcal{L}}_\eta\hat{\mathcal{L}}_\zeta\big) = {}& \mathbf{d}^{\mathsf{T}}L_\eta^{(2)}V\mathbf{L}_\zeta^{(1)} + i\mathbf{d}^{\mathsf{T}}L_\eta^{(2)}\Omega\mathbf{L}_\zeta^{(1)} + 2\mathbf{d}^{\mathsf{T}}L_\eta^{(2)}VL_\zeta^{(2)}\mathbf{d} + 2i\mathbf{d}^{\mathsf{T}}L_\eta^{(2)}\Omega L_\zeta\mathbf{d} + \mathbf{d}^{\mathsf{T}}L_\zeta^{(2)}V\mathbf{L}_\eta^{(1)} + i\mathbf{L}_\eta^{(1)\mathsf{T}}\Omega L_\zeta^{(2)}\mathbf{d} \\
& + 2i\,\mathrm{tr}\big(\Omega L_\zeta^{(2)}VL_\eta^{(2)}\big) + \tfrac{1}{2}\mathrm{tr}\big(VL_\zeta^{(2)}VL_\eta^{(2)}\big) + \tfrac{1}{2}\mathrm{tr}\big(\Omega L_\zeta^{(2)}\Omega L_\eta^{(2)}\big) + \tfrac{1}{2}\mathbf{L}_\eta^{(1)}V\mathbf{L}_\zeta^{(1)} + \tfrac{i}{2}\mathbf{L}_\eta^{(1)\mathsf{T}}\Omega\mathbf{L}_\zeta^{(1)}.
\end{aligned} \tag{A14}
$$

Now, since for any two Hermitian operators $\hat{A}$ and $\hat{B}$ it holds that $2\mathrm{tr}(\hat{\rho}_{\{\mu\}}\hat{A}\hat{B}) = \mathrm{tr}(\hat{\rho}_{\{\mu\}}\{\hat{A},\hat{B}\}_{+}) + \mathrm{tr}(\hat{\rho}_{\{\mu\}}[\hat{A},\hat{B}])$, we find

$$\mathrm{Re}\{\mathrm{tr}(\hat{\rho}_{\{\mu\}}\hat{\mathcal{L}}_\eta\hat{\mathcal{L}}_\zeta)\} = \tfrac{1}{2}\mathrm{tr}(\hat{\rho}_{\{\mu\}}\{\hat{\mathcal{L}}_\eta,\hat{\mathcal{L}}_\zeta\}_{+}) = \mathcal{F}_{\eta\zeta} = \mathcal{F}_{\zeta\eta}, \tag{A15}$$

$$\mathrm{Im}\{\mathrm{tr}(\hat{\rho}_{\{\mu\}}\hat{\mathcal{L}}_\eta\hat{\mathcal{L}}_\zeta)\} = \tfrac{1}{2i}\mathrm{tr}(\hat{\rho}_{\{\mu\}}[\hat{\mathcal{L}}_\eta,\hat{\mathcal{L}}_\zeta]) = \mathcal{J}_{\eta\zeta} = -\mathcal{J}_{\zeta\eta}. \tag{A16}$$

Using the cyclic property of the trace and the identity $\partial_\zeta V = V L_\zeta^{(2)} V + \Omega L_\zeta^{(2)} \Omega$ [32], we have that

$$\tfrac{1}{2}\mathrm{tr}\big(V L_\zeta^{(2)} V L_\eta^{(2)}\big) + \tfrac{1}{2}\mathrm{tr}\big(\Omega L_\zeta^{(2)} \Omega L_\eta^{(2)}\big) = \mathrm{tr}\big(\partial_\zeta V L_\eta^{(2)}\big) = \mathrm{tr}\big(\partial_\eta V L_\zeta^{(2)}\big), \tag{A17}$$

therefore, for Eq. (A15), we can write

$$\mathrm{Re}\{\mathrm{tr}(\hat{\rho}_{\{\mu\}}\hat{\mathcal{L}}_\eta\hat{\mathcal{L}}_\zeta)\} = \mathbf{d}^{\mathsf{T}}L_\eta^{(2)}V\mathbf{L}_\zeta^{(1)} + 2\mathbf{d}^{\mathsf{T}}L_\eta^{(2)}VL_\zeta^{(2)}\mathbf{d} + \mathbf{d}^{\mathsf{T}}L_\zeta^{(2)}V\mathbf{L}_\eta^{(1)} + \tfrac{1}{2}\mathrm{tr}(\partial_\zeta V L_\eta^{(2)}) + \tfrac{1}{2}\mathbf{L}_\eta^{(1)}V\mathbf{L}_\zeta^{(1)}. \tag{A18}$$

Finally, substituting in the expression for $\mathbf{L}^{(1)}$ given by Eq. (18), and adopting in what follows the shorthand notation $\boldsymbol{d}_\zeta \equiv \partial_\zeta \mathbf{d}$, we get

$$\begin{aligned}
\mathrm{Re}\big\{\mathrm{tr}\big(\hat{\rho}_{\{\mu\}}\hat{\mathcal{L}}_\eta\hat{\mathcal{L}}_\zeta\big)\big\} &= 2\mathbf{d}^{\mathsf{T}}L_\eta^{(2)}\boldsymbol{d}_\zeta - 2\mathbf{d}^{\mathsf{T}}L_\eta^{(2)}VL_\zeta^{(2)}\mathbf{d} + 2\mathbf{d}^{\mathsf{T}}L_\eta^{(2)}VL_\zeta^{(2)}\mathbf{d} + 2\mathbf{d}^{\mathsf{T}}L_\zeta^{(2)}\boldsymbol{d}_\eta - 2\mathbf{d}^{\mathsf{T}}L_\zeta^{(2)}VL_\eta^{(2)}\mathbf{d} + \tfrac{1}{2}\mathrm{tr}(\partial_\zeta V L_\eta^{(2)}) \\
&\quad + 2\boldsymbol{d}_\eta^{\mathsf{T}}V^{-1}\boldsymbol{d}_\zeta - 2\boldsymbol{d}_\eta^{\mathsf{T}}L_\zeta^{(2)}\mathbf{d} - 2\mathbf{d}^{\mathsf{T}}L_\eta^{(2)}\boldsymbol{d}_\zeta + 2\mathbf{d}^{\mathsf{T}}L_\eta^{(2)}VL_\zeta^{(2)}\mathbf{d} \\
&= \tfrac{1}{2}\mathrm{tr}\big(\partial_\zeta V L_\eta^{(2)}\big) + 2\boldsymbol{d}_\eta^{\mathsf{T}}V^{-1}\boldsymbol{d}_\zeta \\
&= \mathcal{F}_{\eta\zeta}.
\end{aligned} \tag{A19}$$

Similarly, for Eq. (A16) we have

$$\begin{aligned}
\mathrm{Im}\{\mathrm{tr}(\hat{\rho}_{\{\mu\}}\hat{\mathcal{L}}_\eta\hat{\mathcal{L}}_\zeta)\} &= \mathbf{d}^{\mathsf{T}}L_\eta^{(2)}\Omega\mathbf{L}_\zeta^{(1)} + 2\mathbf{d}^{\mathsf{T}}L_\eta^{(2)}\Omega L_\zeta^{(2)}\mathbf{d} + \mathbf{L}_\eta^{(1)\mathsf{T}}\Omega L_\zeta^{(2)}\mathbf{d} + 2\mathrm{tr}\big(\Omega L_\zeta^{(2)}V L_\eta^{(2)}\big) + \tfrac{1}{2}\mathbf{L}_\eta^{(1)\mathsf{T}}\Omega\mathbf{L}_\zeta^{(1)} \\
&= 2\mathbf{d}^{\mathsf{T}}L_\eta^{(2)}\Omega V^{-1}\boldsymbol{d}_\zeta - 2\mathbf{d}^{\mathsf{T}}L_\eta^{(2)}\Omega V^{-1}\boldsymbol{d}_\zeta + 2L_\eta^{(2)}\Omega L_\zeta^{(2)}\mathbf{d} + 2\boldsymbol{d}_\eta^{\mathsf{T}}V^{-1}\Omega L_\zeta^{(2)}\mathbf{d} - 2\mathbf{d}^{\mathsf{T}}L_\eta^{(2)}\Omega L_\zeta^{(2)}\mathbf{d} \\
&\quad + 2\mathrm{tr}\big(\Omega L_\zeta^{(2)}V L_\eta^{(2)}\big) + 2\boldsymbol{d}_\eta^{\mathsf{T}}V^{-1}\Omega V^{-1}\boldsymbol{d}_\zeta - 2\boldsymbol{d}_\eta^{\mathsf{T}}V^{-1}\Omega L_\zeta^{(2)}\mathbf{d} - 2\mathbf{d}^{\mathsf{T}}L_\eta^{(2)}\Omega V^{-1}\boldsymbol{d}_\zeta + 2\mathbf{d}^{\mathsf{T}}L_\eta^{(2)}\Omega L_\zeta^{(2)}\mathbf{d} \\
&= 2\mathrm{tr}\big(\Omega L_\zeta^{(2)}V L_\eta^{(2)}\big) + 2\boldsymbol{d}_\eta^{\mathsf{T}}V^{-1}\Omega V^{-1}\boldsymbol{d}_\zeta \\
&= \mathcal{J}_{\eta\zeta}.
\end{aligned} \tag{A20}$$

In conclusion, to summarize, we have shown that

$$\mathrm{tr}(\hat{\rho}_{\{\mu\}}\hat{\mathcal{L}}_\eta\hat{\mathcal{L}}_\zeta) = \mathcal{F}_{\eta\zeta} + i\mathcal{J}_{\eta\zeta}, \tag{A21}$$

with

$$\mathcal{F}_{\eta\zeta} = \tfrac{1}{2}\mathrm{tr}\big(\partial_\zeta V L_\eta^{(2)}\big) + 2\boldsymbol{d}_\eta^{\mathsf{T}}V^{-1}\boldsymbol{d}_\zeta, \tag{A22}$$

$$\mathcal{J}_{\eta\zeta} = 2\mathrm{tr}\big(\Omega L_\zeta^{(2)}V L_\eta^{(2)}\big) + 2\boldsymbol{d}_\eta^{\mathsf{T}}V^{-1}\Omega V^{-1}\boldsymbol{d}_\zeta. \tag{A23}$$

This completes the proof of Theorem 1.

APPENDIX B: ADDITIONAL DETAILS ON THE ESTIMATION PROBLEM OF FIGURE 1

For completeness, here we include the analytical expression of the QFI matrix for estimating the three parameters $\{\phi, x, y\}$ as described in Fig. 1, using an input TMDSS $\hat{\rho}_0$ of the form given by Eq. (22), with $r \geqslant 0$, $\mathrm{Re}[\alpha] = \mathrm{Re}[\beta] = 0$, and $\mathrm{Im}[\alpha] = \mathrm{Im}[\beta]$.

The QFI matrix for the considered problem takes the form

$$\mathcal{F} = \begin{pmatrix} \mathcal{F}_{\phi\phi} & \mathcal{F}_{\phi x} & \mathcal{F}_{\phi y} \\ \mathcal{F}_{\phi x} & \mathcal{F}_{xx} & \mathcal{F}_{xy} \\ \mathcal{F}_{\phi y} & \mathcal{F}_{xy} & \mathcal{F}_{yy} \end{pmatrix}, \tag{B1}$$

where, using Eq. (20), we have

$$\mathcal{F}_{\phi\phi} = \frac{2|\alpha|^2 x[x\sinh(2r) + x\cosh(2r) + y]}{2xy\cosh(2r) + x^2 + y^2},$$

$$\mathcal{F}_{xx} = \frac{1}{2x^2}\left\{\frac{(x^2 - y^2 + 1)^2}{2xy\cosh(2r) + x^2 + y^2 - 1} - \frac{[(x-y)^2 + 1][(x+y)^2 + 1]}{2xy\cosh(2r) + x^2 + y^2 + 1} + \frac{4|\alpha|^2 x}{x+y} + 2\right\} + \frac{2|\alpha|^2(e^{2r} - 1)}{(x+y)(e^{2r}y + x)},$$

$$\mathcal{F}_{yy} = \frac{2\left[x^2\cosh(4r) + 2xy\cosh(2r) + y^2 + 1\right]}{2xy\left[2\cosh(2r)\left(x^2 + y^2\right) + xy\cosh(4r)\right] + x^4 + 4x^2y^2 + y^4 - 1},$$

$$\mathcal{F}_{\phi x} = 0,$$

$$\mathcal{F}_{\phi y} = 0,$$

$$\mathcal{F}_{xy} = \frac{2\left(x^2 + y^2 + 1\right)\cosh(2r) + 4xy}{2xy\left[2\cosh(2r)\left(x^2 + y^2\right) + xy\cosh(4r)\right] + x^4 + 4x^2y^2 + y^4 - 1}.$$

In the high input energy limit, $\bar{n} = \sinh^2(r) + |\alpha|^2 \gg 0$, the QFI matrix (B1) can be approximated as

$$\mathcal{F} \approx \begin{pmatrix} \frac{2px\bar{n}}{y} + c_\phi & 0 & 0 \\ 0 & \frac{2p\bar{n}}{xy} + c_x & O(\bar{n}^{-1}) \\ 0 & O(\bar{n}^{-1}) & \frac{1}{y^2} \end{pmatrix}, \tag{B2}$$

where c_ϕ and c_x are some constants. From this we see that the nonzero off-diagonal term scales as $\mathcal{F}_{xy} \sim \bar{n}^{-1}$, thus vanishing in the limit $\bar{n} \gg 0$, in which case the compatibility condition (iii) is asymptotically fulfilled, as stated in Sec. IV. We also see that the variances on estimating ϕ and x scale as the standard quantum limit, $\{\mathcal{F}_{\phi\phi}^{-1}, \mathcal{F}_{xx}^{-1}\} \sim \bar{n}^{-1}$, while the variance on estimating the added noise y tends to a constant depending on the parameter itself, $\mathcal{F}_{yy}^{-1} \sim y^2$.

Optimizing the input state for each parameter independently in individual estimation

The analysis of the metrological scheme in Fig. 1 provided in Sec. IV compares the strategies of estimating each parameter individually and estimating them simultaneously. For simplicity of presentation, the analysis of individual estimation presented in Sec. IV in fact optimizes the minimal total combined ("com") variance associated with the estimation of the three parameters over the family of input states, i.e.,

$$\Delta_{\text{opt}}^{\text{ind}} \equiv \Delta_{\text{opt}}^{\text{ind,com}} = \min_{\hat{\rho}_0} \sum_{\eta \in \{\mu\}} \mathcal{F}_{\eta\eta}^{-1}. \tag{B3}$$

Realistically, one may expect that in such an estimation procedure, as each parameter is estimated in an independent experiment, a different optimal input state could be determined for each parameter and used in each corresponding experiment. This would, in principle, lead to a smaller total variance, resulting from the sum of the minimal variances optimized independently ("ind") for each parameter, thus altering our optimization to the following:

$$\Delta_{\text{opt}}^{\text{ind,ind}} = \sum_{\eta \in \{\mu\}} \Delta_{\text{opt}}^{\eta} = \sum_{\eta \in \{\mu\}} \min_{\hat{\rho}_0} \mathcal{F}_{\eta\eta}^{-1}. \tag{B4}$$

We present here the results of this independent optimization, finding that a slight improvement in the ensuing individual estimation strategy is obtained but the conceptual conclusions reached in Sec. IV, including the qualitative comparison with the simultaneous estimation strategy, remain unchanged.

As stated in Sec. IV, the compatibility condition (i) depends only on the displacement of the initial state and may be written as $|\alpha|^2 = |\beta|^2$. In Sec. IV, it is also found that the minimum combined variance $\Delta_{\text{opt}}^{\text{ind,com}}$, as defined in Eq. (B3), is achieved with states that have $\text{Re}[\alpha] = \text{Re}[\beta] = 0$ and $\text{Im}[\alpha] = \text{Im}[\beta]$. We find that these same conditions minimize each independent variance Δ^η, so that also the quantity $\Delta_{\text{opt}}^{\text{ind,ind}}$ defined in Eq. (B4) is minimized and the compatibility condition remains obeyed.
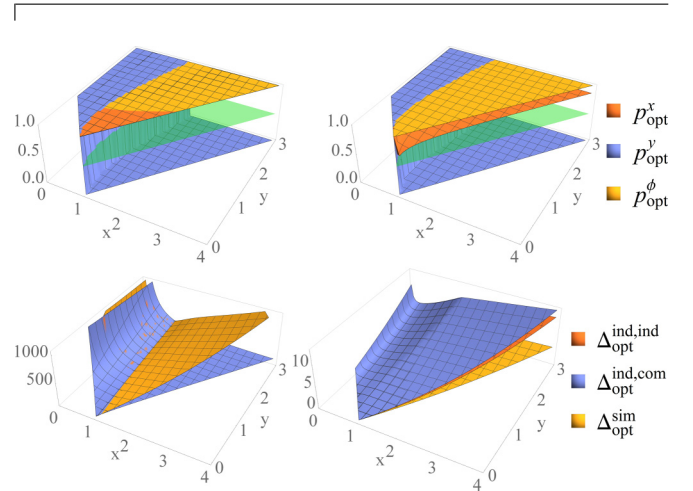

FIG. 3. Comparing optimizing the input state for each parameter independently ("ind, ind"), to optimizing for the combined error ("ind, com"), as in Fig. 2. Left column: Analysis at low energy, $\bar{n} = 0.005$. Right column: Analysis at higher energy, $\bar{n} = 5$. Top: Optimal proportion of input energy to put in the displacement, p_{opt}, comparing individual estimations of each parameter. The unmeshed (green online) plane marks $p_{\text{opt}} = 1/2$, above which more energy should be used for displacement than squeezing. Bottom: Minimal achievable error Δ_{opt} for the introduced independent estimation, in comparison with the two strategies discussed in Sec. IV. All the presented results are independent of the value of the unknown phase ϕ. All the quantities plotted are dimensionless.

The proportion of the energy p_{opt} to dedicate to the displacement of the initial state (as opposed to squeezing the state) for minimizing the combined error is discussed in Sec. IV and shown in Fig. 2 (top). This quantity changes when considering the errors optimized for each parameter independently, as shown in Fig. 3 (top). We find that to estimate ϕ one should always have all energy in the displacement. For estimating x, there exists a boundary in the parameter space, either side of which all energy should go to displacement or all energy should go to squeezing. As the total energy is increased, this boundary

shifts as more of the parameter space favors squeezed probes over displaced probes. At low energy, to estimate y, all energy should be dedicated to displacement, while as the energy is increased the ratio p_{opt} varies but never drops below $1/2$, so more energy should always be dedicated to displacement than squeezing.

This shows a difference from minimizing the combined error. In Fig. 3 (bottom), we explore the effect this has on the total minimum error. We find that, as Δ_{opt}^{ϕ} dominates, $\Delta_{opt}^{ind,ind}$ is only slightly smaller than $\Delta_{opt}^{ind,com}$, therefore the refinement of the individual estimation scheme investigated here has *de facto* very little effect on the total error and the behavior it displays. We therefore conclude that using $\Delta_{opt}^{ind} \equiv \Delta_{opt}^{ind,com}$ is adequate for discussing the qualities of the individual estimation scheme in the analyzed example, as is done in Sec. IV.

---

[1] C. M. Caves, Quantum-mechanical noise in an interferometer, Phys. Rev. D **23**, 1693 (1981).

[2] S. F. Huelga, C. Macchiavello, T. Pellizzari, A. K. Ekert, M. B. Plenio, and J. I. Cirac, Improvement of Frequency Standards with Quantum Entanglement, Phys. Rev. Lett. **79**, 3865 (1997).

[3] V. Giovannetti, S. Lloyd, and L. Maccone, Quantum Metrology, Phys. Rev. Lett. **96**, 010401 (2006).

[4] M. G. A. Paris, Quantum estimation for quantum technology, Int. J. Quant. Inf. **07**, 125 (2009).

[5] V. Giovannetti, S. Lloyd, and L. Maccone, Advances in quantum metrology, Nat. Photonics **5**, 222 (2011).

[6] J. P. Dowling and K. P. Seshadreesan, Quantum optical technologies for metrology, sensing, and imaging, J. Lightwave Technol. **33**, 2359 (2015).

[7] G. Tóth and I. Apellaniz, Quantum metrology from a quantum information science perspective, J. Phys. A: Math. Theor. **47**, 424006 (2014).

[8] M. Szczykulska, T. Baumgratz, and A. Datta, Multi-parameter quantum metrology, Adv. Phys.: X **1**, 621 (2016).

[9] L. Pezzè, A. Smerzi, M. K. Oberthaler, R. Schmied, and P. Treutlein, Non-classical states of atomic ensembles: Fundamentals and applications in quantum metrology, arXiv:1609.01609 [Rev. Mod. Phys. (to be published)].

[10] D. Braun, G. Adesso, F. Benatti, R. Floreanini, U. Marzolino, M. W. Mitchell, and S. Pirandola, Quantum enhanced measurements without entanglement, arXiv:1701.05152 [Rev. Mod. Phys. (to be published)].

[11] V. Giovannetti, S. Lloyd, and L. Maccone, Quantum-enhanced measurements: Beating the standard quantum limit, Science **306**, 1330 (2004).

[12] H. Katori, Optical lattice clocks and quantum metrology, Nat. Photonics **5**, 203 (2011).

[13] R. Schnabel, N. Mavalvala, D. E. McClelland, and P. K. Lam, Quantum metrology for gravitational wave astronomy, Nat. Commun. **1**, 121 (2010).

[14] J. Aasi *et al.*, Enhanced sensitivity of the LIGO gravitational wave detector by using squeezed states of light, Nat. Photonics **7**, 613 (2013).

[15] M. Aspachs, G. Adesso, and I. Fuentes, Optimal Quantum Estimation of the Unruh-Hawking Effect, Phys. Rev. Lett. **105**, 151301 (2010).

[16] M. Ahmadi, D. E. Bruschi, and I. Fuentes, Quantum metrology for relativistic quantum fields, Phys. Rev. D **89**, 065028 (2014).

[17] J. Cai and M. B. Plenio, Chemical Compass Model for Avian Magnetoreception as a Quantum Coherent Device, Phys. Rev. Lett. **111**, 230503 (2013).

[18] P. Kómár, E. M. Kessler, M. Bishof, L. Jiang, A. S. Sørensen, J. Ye, and M. D. Lukin, A quantum network of clocks, Nat. Phys. **10**, 582 (2014).

[19] A. N. Boto, P. Kok, D. S. Abrams, S. L. Braunstein, C. P. Williams, and J. P. Dowling, Quantum Interferometric Optical Lithography: Exploiting Entanglement to Beat the Diffraction Limit, Phys. Rev. Lett. **85**, 2733 (2000).

[20] L. A. Correa, M. Mehboudi, G. Adesso, and A. Sanpera, Individual Quantum Probes for Optimal Thermometry, Phys. Rev. Lett. **114**, 220405 (2015).

[21] A. De Pasquale, D. Rossini, R. Fazio, and V. Giovannetti, Local quantum thermal susceptibility, Nat. Commun. **7**, 12782 (2016).

[22] S. Schmitt, T. Gefen, F. M. Stürner, T. Unden, G. Wolff, C. Müller, J. Scheuer, B. Naydenov, M. Markham, S. Pezzagna, J. Meijer, I. Schwarz, M. Plenio, A. Retzker, L. P. McGuinness, and F. Jelezko, Submillihertz magnetic spectroscopy performed with a nanoscale quantum sensor, Science **356**, 832 (2017).

[23] J. M. Boss, K. S. Cujia, J. Zopes, and C. L. Degen, Quantum sensing with arbitrary frequency resolution, Science **356**, 837 (2017).

[24] M. Tsang, R. Nair, and X.-M. Lu, Quantum Theory of Superresolution for Two Incoherent Optical Point Sources, Phys. Rev. X **6**, 031033 (2016).

[25] R. Nair and M. Tsang, Far-Field Superresolution of Thermal Electromagnetic Sources at the Quantum Limit, Phys. Rev. Lett. **117**, 190801 (2016).

[26] C. Lupo and S. Pirandola, Ultimate Precision Bound of Quantum and Subwavelength Imaging, Phys. Rev. Lett. **117**, 190802 (2016).

[27] M. A. Taylor and W. P. Bowen, Quantum metrology and its application in biology, arXiv:1409.0950v2.

[28] C. Bonato, M. S. Blok, H. T. Dinani, D. W. Berry, M. L. Markham, D. J. Twitchen, and R. Hanson, Optimized quantum sensing with a single electron spin using real-time adaptive measurements, Nat. Nanotech. **11**, 247 (2015).

[29] S. L. Braunstein and P. van Loock, Quantum information with continuous variables, Rev. Mod. Phys. **77**, 513 (2005).

[30] C. Weedbrook, S. Pirandola, R. García-Patrón, N. J. Cerf, T. C. Ralph, J. H. Shapiro, and S. Lloyd, Gaussian quantum information, Rev. Mod. Phys. **84**, 621 (2012).

[31] G. Adesso, S. Ragy, and A. R. Lee, Continuous variable quantum information: Gaussian states and beyond, Open Syst. Inf. Dyn. **21**, 1440001 (2014).

[32] A. Serafini, *Quantum Continuous Variables: A Primer of Theoretical Methods* (Taylor & Francis, Oxford, 2017).

[33] A. Monras, Optimal phase measurements with pure Gaussian states, Phys. Rev. A **73**, 033821 (2006).

[34] A. Monras and M. G. A. Paris, Optimal Quantum Estimation of Loss in Bosonic Channels, Phys. Rev. Lett. **98**, 160401 (2007).

[35] G. Adesso, F. Dell'Anno, S. De Siena, F. Illuminati, and L. A. M. Souza, Optimal estimation of losses at the ultimate quantum limit with non-Gaussian states, Phys. Rev. A **79**, 040305 (2009).

[36] R. Gaiba and M. G. A. Paris, Squeezed vacuum as a universal quantum probe, Phys. Lett. A **373**, 934 (2009).

[37] B. Bellomo, A. De Pasquale, G. Gualdi, and U. Marzolino, Reconstruction of Markovian master equation parameters through symplectic tomography, Phys. Rev. A **80**, 052108 (2009).

[38] M. G. Genoni, M. G. A. Paris, G. Adesso, H. Nha, P. L. Knight, and M. S. Kim, Optimal estimation of joint parameters in phase space, Phys. Rev. A **87**, 012107 (2013).

[39] A. Monras and F. Illuminati, Measurement of damping and temperature: Precision bounds in Gaussian dissipative channels, Phys. Rev. A **83**, 012315 (2011).

[40] O. Pinel, J. Fade, D. Braun, P. Jian, N. Treps, and C. Fabre, Ultimate sensitivity of precision measurements with intense Gaussian quantum light: A multimodal approach, Phys. Rev. A **85**, 010101 (2012).

[41] O. Pinel, P. Jian, N. Treps, C. Fabre, and D. Braun, Quantum parameter estimation using general single-mode Gaussian states, Phys. Rev. A **88**, 040102 (2013).

[42] A. Monras, Phase space formalism for quantum estimation of Gaussian states, arXiv:1303.3682.

[43] Y. Gao and H. Lee, Bounds on quantum multiple-parameter estimation with Gaussian state, Eur. Phys. J. D **68**, 347 (2014).

[44] Z. Jiang, Quantum Fisher information for states in exponential form, Phys. Rev. A **89**, 032128 (2014).

[45] D. Šafránek, A. R. Lee, and I. Fuentes, Quantum parameter estimation using multi-mode Gaussian states, New J. Phys. **17**, 073016 (2015).

[46] N. Friis, M. Skotiniotis, I. Fuentes, and W. Dür, Heisenberg scaling in Gaussian quantum metrology, Phys. Rev. A **92**, 022106 (2015).

[47] L. Banchi, S. L. Braunstein, and S. Pirandola, Quantum Fidelity for Arbitrary Gaussian States, Phys. Rev. Lett. **115**, 260501 (2015).

[48] L. Rigovacca, A. Farace, A. De Pasquale, and V. Giovannetti, Gaussian discriminating strength, Phys. Rev. A **92**, 042331 (2015).

[49] R. Demkowicz-Dobrzański, M. Jarzyna, and J. Kolodyński, Chapter Four—Quantum limits in optical interferometry, in *Progress in Optics*, edited by E. Wolf (Elsevier, New York, 2015), Vol. 60, p. 345.

[50] D. Šafránek and I. Fuentes, Optimal probe states for the estimation of Gaussian unitary channels, Phys. Rev. A **94**, 062313 (2016).

[51] P. Marian and T. A. Marian, Quantum Fisher information on two manifolds of two-mode Gaussian states, Phys. Rev. A **93**, 052330 (2016).

[52] K. Duivenvoorden, B. M. Terhal, and D. Weigand, Single-mode displacement sensor, Phys. Rev. A **95**, 012305 (2017).

[53] C. N. Gagatsos, D. Branford, and A. Datta, Gaussian systems for quantum-enhanced multiple phase estimation, Phys. Rev. A **94**, 042342 (2016).

[54] J. Liu, X.-M. Lu, Z. Sun, and X. Wang, Quantum multiparameter metrology with generalized entangled coherent state, J. Phys. A: Math. Theor. **49**, 115302 (2016).

[55] S. Ragy, M. Jarzyna, and R. Demkowicz-Dobrzański, Compatibility in multiparameter quantum metrology, Phys. Rev. A **94**, 052108 (2016).

[56] M. E. Pearce, E. T. Campbell, and P. Kok, Optimal quantum metrology of distant black bodies, Quantum **1**, 21 (2017).

[57] Q. Zhuang, Z. Zhang, and J. H. Shapiro, Entanglement-enhanced lidars for simultaneous range and velocity measurements, Phys. Rev. A **96**, 040304 (2017).

[58] T. J. Proctor, P. A. Knott, and J. A. Dunningham, Multiparameter Estimation in Networked Quantum Sensors, Phys. Rev. Lett. **120**, 080501 (2018).

[59] S. Pirandola and C. Lupo, Ultimate Precision of Adaptive Noise Estimation, Phys. Rev. Lett. **118**, 100502 (2017).

[60] C. Helstrom, Minimum mean-squared error of estimates in quantum statistics, Phys. Lett. A **25**, 101 (1967).

[61] S. L. Braunstein and C. M. Caves, Statistical Distance and the Geometry of Quantum States, Phys. Rev. Lett. **72**, 3439 (1994).

[62] K. Matsumoto, A new approach to the Cramér-Rao-type bound of the pure-state model, J. Phys. A: Math. Gen. **35**, 3111 (2002).

[63] A. Monras and F. Illuminati, Information geometry of Gaussian channels, Phys. Rev. A **81**, 062326 (2010).

[64] A. Ferraro, S. Olivares, and M. G. A. Paris, *Gaussian States in Quantum Information* (Bibliopolis, Napoli, 2005).

[65] R. Simon, N. Mukunda, and B. Dutta, Quantum-noise matrix for multimode systems: U(n) invariance, squeezing, and normal forms, Phys. Rev. A **49**, 1567 (1994).

[66] C. M. Caves and P. D. Drummond, Quantum limits on bosonic communication rates, Rev. Mod. Phys. **66**, 481 (1994).

[67] M. M. Wolf, D. Pérez-García, and G. Giedke, Quantum Capacities of Bosonic Channels, Phys. Rev. Lett. **98**, 130501 (2007).

[68] J. Schäfer, E. Karpov, R. García-Patrón, O. V. Pilyavets, and N. J. Cerf, Equivalence Relations for the Classical Capacity of Single-Mode Gaussian Quantum Channels, Phys. Rev. Lett. **111**, 030503 (2013).

[69] A. Mari, V. Giovannetti, and A. S. Holevo, Quantum state majorization at the output of bosonic Gaussian channels, Nat. Commun. **5**, 3826 (2014).

[70] V. Giovannetti, R. García-Patrón, N. J. Cerf, and A. S. Holevo, Ultimate classical communication rates of quantum optical channels, Nat. Photonics **8**, 796 (2014).

[71] C. Vaneph, T. Tufarelli, and M. G. Genoni, Quantum estimation of a two-phase spin rotation, Quantum Meas. Quantum Metrol. **1**, 12 (2013).

[72] R. D. Gill and M. Guta, On asymptotic quantum statistical inference, in *From probability to statistics and back: High-dimensional models and processes – A Festschrift in honor of Jon A. Wellner* (Institute of Mathematical Statistics, Beachwood, OH, 2013), p. 105.

[73] P. C. Humphreys, M. Barbieri, A. Datta, and I. A. Walmsley, Quantum Enhanced Multiple Phase Estimation, Phys. Rev. Lett. **111**, 070403 (2013).

[74] P. J. D. Crowley, A. Datta, M. Barbieri, and I. A. Walmsley, Tradeoff in simultaneous quantum-limited phase and loss estimation in interferometry, Phys. Rev. A **89**, 023845 (2014).

[75] L. Pezzè, M. A. Ciampini, N. Spagnolo, P. C. Humphreys, A. Datta, I. A. Walmsley, M. Barbieri, F. Sciarrino, and A. Smerzi, Optimal Measurements for Simultaneous Quantum Estimation of Multiple Phases, Phys. Rev. Lett. **119**, 130504 (2017).

[76] R. Yousefjani, R. Nichols, S. Salimi, and G. Adesso, Estimating phase with a random generator: Strategies and resources in

multiparameter quantum metrology, Phys. Rev. A **95**, 062307 (2017).

[77] L. Banchi (private communication).

[78] A. Serafini, G. Adesso, and F. Illuminati, Unitarily localizable entanglement of Gaussian states, Phys. Rev. A **71**, 032349 (2005).

[79] S. Pirandola, A. Serafini, and S. Lloyd, Correlation matrices of two-mode bosonic systems, Phys. Rev. A **79**, 052327 (2009).

[80] L. Mišta and K. Baksová, Gaussian intrinsic entanglement for states with partial minimum uncertainty, Phys. Rev. A **97**, 012305 (2018).

[81] B. M. Escher, R. L. de Matos Filho, and L. Davidovich, General framework for estimating the ultimate precision limit in noisy quantum-enhanced metrology, Nat. Phys. **7**, 406 (2011).

[82] R. Demkowicz-Dobrzański, J. Kolodyński, and M. Guta, The elusive Heisenberg limit in quantum-enhanced metrology, Nat. Commun. **3**, 1063 (2012).

[83] Special instances of this problem have been considered in the literature, where the estimation of only one or two such parameters was addressed [1,5,33–36,39,41,43,53,55,59].

[84] Notice that $\mathcal{F}_{\phi x} = \mathcal{F}_{\phi y} = 0$, but in general $\mathcal{F}_{xy} \neq 0$ (see Appendix A).

[85] F. Fröwis, M. Skotiniotis, B. Kraus, and W. Dür, Optimal quantum states for frequency estimation, New J. Phys. **16**, 083010 (2014).

[86] P. A. Knott, A search algorithm for quantum state engineering and metrology, New J. Phys. **18**, 073033 (2016).

[87] D. Šafránek, Calculating optimal bounds on the multi-parameter estimation of Gaussian quantum states, arXiv:1801.00299.